Conversion of a soluble protein into a potent chaperone *in vivo*

Short title: Intrinsic chaperone activity of a soluble protein

Soon Bin Kwon[1], Kisun Ryu[1], Ahyun Son[1], Hotcherl Jeong[2], Keo-Heun Lim[3], Kyun-Hwan Kim[3], Baik L. Seong[1,4,*], & Seong Il Choi [5,*]

[1] Department of Biotechnology, College of Life Science and Biotechnology, Yonsei University, Seoul 03722, Republic of Korea

[2] Department of Pharmacy, Ewha Womans University, Seoul 03760, Republic of Korea

[3] Department of Pharmacology, Center for Cancer Research and Diagnostic Medicine, IBST, School of Medicine, Konkuk University, Seoul 05029, Republic of Korea

[4] Vaccine Translational Research Center (VTRC), Yonsei University, Seoul 03722, Republic of Korea

[5] Department of Biochemistry and Biophysics, Stockholm University, SE-106 91 Stockholm, Sweden.

* Corresponding authors

Correspondence should be addressed to S.I.C. (choisi345@gmail.com) or B.L.S. (blseong@yonsei.ac.kr).

Abstract

Protein-folding assistance and aggregation inhibition by cellular factors are largely understood in the context of molecular chaperones. As an alternative and complementary model, we previously proposed that, in general, soluble cellular macromolecules including chaperones with large excluded volume and surface charges exhibit the intrinsic chaperone activity to prevent aggregation of their connected polypeptides, irrespective of the connection types, and thus to aid productive protein folding. As a proof of concept, we here demonstrated that a model soluble protein with an inactive protease domain robustly exerted chaperone activity toward various proteins harboring a short protease-recognition tag of 7 residues in *Escherichia coli*. The chaperone activity of this protein was similar or even superior to that of representative *E. coli* chaperones *in vivo*. Furthermore, *in vitro* refolding experiments confirmed the *in vivo* results. Our findings revealed that a soluble protein exhibits the intrinsic chaperone activity, which is manifested, upon binding to aggregation-prone proteins. This study gives new insights into the ubiquitous chaperoning role of cellular macromolecules in protein-folding assistance and aggregation inhibition underlying the maintenance of protein solubility and proteostasis *in vivo*.

Abbreviations

Ap1m2	AP-1 complex subunit mu-2
DnaKJE	DnaK-DnaJ-GrpE
EGFP	Enhanced Green Fluorescent Protein
GCSF	Granulocyte colony stimulating factor
GroELS	GroEL-GroES
HBx	Hepatitis B virus X protein
hMDH	Malate Dehydrogenase from *Homo sapiens*
HSP	Heat Shock Protein
IPTG	isopropyl β-D-1-thiogalactopyranoside
mTEV	Tobacco etch virus protease domain with C151A mutation
mTEVsw	Tobacco etch virus protease domain variant with C151A mutation
RS	Lysyl-tRNA synthetase of *Escherichia coli*
SDS-PAGE	Sodium dodecyl sulfate polyacrylamide gel electrophoresis
TF	Trigger Factor

Introduction

How metastable proteins with respect to aggregation fold efficiently and maintain their solubility in the crowded cellular environment has been a fundamental yet unsolved question in biology [1-4]. Protein aggregation is closely associated with the numerous human disorders, including neurodegeneration [5]. Molecular chaperones and principles underlying their action mechanisms have provided the conceptual frameworks for understanding of protein-folding assistance, aggregation inhibition, and proteostasis *in vivo* [6, 7]. However, chaperones are ineffective for numerous aggregation-prone proteins [8], and they need to be understood with caveats, given accumulating evidence. Chaperones generally assist protein folding by preventing off-pathway "intermolecular" aggregation (or increasing the final folding yield), often at the expense of the "intramolecular" folding rate or thermodynamic stability of substrate proteins [9-11]. By contrast, in some cases, chaperones can increase the folding rate of client proteins as folding catalysts [12-14]. Both action mechanisms of chaperones are basically different although they are not mutually exclusive.

Chaperones commonly recognize and bind to the exposed hydrophobic residues of non-native or unfolded polypeptides, thereby enabling protein quality control [3, 6, 7]. These findings led to widespread beliefs in 1) the hydrophobic interaction-mediated substrate recognition of chaperones; and 2) such interaction-mediated substrate stabilization against aggregation [3, 4, 7, 15]. However, several lines of evidence challenge these prevailing mechanisms. Chaperones, such as Spy and Trigger Factor (TF), can recognize and bind to the surface-exposed charged regions of substrates [16, 17], and the endoplasmic reticulum lectin chaperones calnexin/calreticulin bind to the carbohydrate parts of their substrate proteins [18]. Moreover, GroEL and TRiC/CCT can also recognize their substrates mainly through electrostatic interactions [19, 20]. These findings naturally raise a fundamental question regarding how chaperones stabilize their substrates, which are connected via non-

hydrophobic interactions, against aggregation. Contrary to such widespread belief, it remains poorly defined what forces (or factors) of chaperones or other cellular macromolecules are responsible for stabilizing their bound substrates against aggregation. This is primarily due to the inherent difficulty of this study, including conformational changes of macromolecules and irreversible aggregation. Intriguingly, the surface-charge patches of heat-shock protein 90 (HSP90) are critical for the anti-aggregation activity for its substrate proteins, although the charge patches are located away from the substrate-binding regions [21]. Similarly, the substrate-stabilizing ability of HSP70 resulted largely from its N-terminal domain rather than its C-terminal substrate-binding domain in the context of covalent fusion [22], suggesting that the substrate-interaction forces of chaperones do not necessarily represent the major substrate-stabilizing forces against aggregation.

We previously proposed a *cis*-acting protein-folding helper system, which appears to operate differently from the classical *trans*-acting chaperones [4, 23]. A hallmark feature of the cellular folding environment is that nascent polypeptides are tethered to the cellular macromolecules, such as ribosomes (2000–3200 kDa), membranes, or cotranslationally folded (or prefolded) domains in multi-domain proteins. *De novo* protein folding on these cellular macromolecules has been a major issue in terms of chaperone function [7, 24-26], but the tethering effect of such macromolecules has long been underappreciated. However, based on the robust chaperone-like activity of these macromolecules, as well as a variety of highly soluble proteins, toward various heterologous aggregation-prone proteins in the fusion context (or in *cis*) [27-30], this *cis*-acting chaperone-like type was proposed to play a pivotal role in the folding and aggregation inhibition of endogenous proteins [23]. Consistent with this *cis*-acting model, several lines of evidence indicate that the cytosol-exposed nascent chains tethered to ribosomes are aggregation-resistant and co-translational folding-competent [31-34]. Remarkably, intermolecular repulsive (or destabilizing) forces, such as electrostatic

and steric repulsions by the surface charges and excluded volume of cellular macromolecules, were proposed to stabilize their tethered polypeptides against aggregation independently of the attractive intermolecular interactions and their effect on the conformational changes, while the tethered polypeptides can fold based on their own sequence information in the absence of adenosine triphosphate (ATP) consumption [4, 23]. This stabilizing mechanism can underlie the intrinsic chaperone activity of soluble macromolecules. The magnitudes of these intermolecular repulsive forces were suggested to increase corresponding to the size and surface charge of the molecules [22, 23]. Importantly, these two forces have been well known as major factors in stabilizing colloids against aggregation [35, 36]. This stabilizing mechanism well explains the surface-charge effect of HSP90 on anti-aggregation, as well as obvious charge effects on protein solubility [4, 23]. Similarly, entropic bristling and hydration by the excluded volume and charged residues of intrinsically disordered proteins or regions were proposed to solubilize their fused proteins [37, 38]. Moreover, the entropic pulling forces of HSP70 resulting from its excluded volume repulsions were proposed to underlie its diverse functions [39]. Nonetheless, so far, the aggregation inhibition by the intermolecular repulsive forces of cellular macromolecules has been largely ignored; instead, the aggregation inhibition has been explained predominantly in the context of the direct attractive interactions between cellular macromolecules and polypeptides. It should be noted that both action mechanisms act independently and simultaneously.

Importantly, large excluded volume and surface charges are the common intrinsic properties of any type of soluble cellular macromolecule including chaperones. This prompted us to hypothesize that cellular macromolecules exhibit the intrinsic chaperone activity, and thus they act as chaperones for their connected polypeptides irrespective of the connection types between them [4, 40]. To test this hypothesis, we here constructed a *trans*-acting artificial chaperone system. Our results revealed that a model soluble protein exhibits

the intrinsic chaperone activity to recapitulate the core features of the classical chaperones, such as aggregation inhibition and folding assistance, upon binding to aggregation-prone proteins in *E. coli*.

Results

Design of an artificial chaperone system *in vivo*

To explore the intrinsic chaperone activity of a soluble protein, we designed an artificial chaperone system in which a model soluble protein (named RS-mTEV) specifically binds to a short flanking tag of 7 residues in the substrate proteins (**Fig 1**). As a substrate-binding module of RS-mTEV, we chose a mutant protease domain of tobacco etch virus (mTEV) with no proteolytic activity, but still maintaining the binding affinity for its canonical recognition sequence (ENLYFQG) [41]. This protease domain is marginally soluble when expressed alone at 37 °C [42]. To increase mTEV solubility, it was fused to the C-terminus of *E. coli* lysyl tRNA synthetase (RS; 57 kDa), which is known to be a solubility-enhancing fusion partner [30], resulting in a more soluble RS-mTEV protein (**S1 Fig**). As a client protein of RS-mTEV, enhanced green fluorescent protein (EGFP) was fused to hepatitis B virus X protein (HBx) with intrinsically disordered regions [43], to yield L-EGFP-HBx where "L" denotes the recognition sequence (ENLYFQG). This model system was designed to minimize the direct binding except for the "L" tag between RS-mTEV and its client protein during folding and aggregation processes to assess the intrinsic RS-mTEV chaperone activity. Moreover, the substrate-binding domain (mTEV) is separated as an independent module from the solubility-enhancing module (RS) in RS-mTEV, providing a unique opportunity to distinguish between the contributions of the two modules to RS-mTEV chaperone function later.

RS-mTEV acts as a potent chaperone for its client proteins *in vivo*

We investigated the effect of RS-mTEV co-expression on both L-EGFP-HBx solubility and folding in *E. coli* using two co-expression vectors. Information about these vectors is described in more detail (**S2 Fig**). RS-mTEV co-expression markedly increased L-EGFP-

156 HBx solubility by ~75%, whereas RS co-expression did not increase the solubility (~16%)
157 similar to the corresponding solubility (~12%) in background cells containing a mock vector
158 pLysE as a control (**Fig 2a**). We further confirmed that a specific binding of RS-mTEV to the
159 "L" tag in L-EGFP-HBx increased the protein solubility. The residue N171 in mTEV is
160 important for the substrate recognition [41]; therefore, this mutation in RS-mTEV [named
161 RS-mTEV(N171A)] resulted in a significantly impaired substrate-binding ability (**S3 Fig**).
162 Correspondingly, RS-mTEV(N171A) had no detectable solubility-enhancing ability for the
163 substrate protein (**Fig 2a**). Similarly, the solubility of L(m)-EGFP-HBx with the mutation in
164 the "L" tag (ENLYFQG to YNLEFQG) did not respond to RS-mTEV co-expression. Other
165 mutations in the conserved recognition sequence of "L" tag consistently resulted in little or
166 no effect on the protein solubility like L(m)-EGFP-HBx (**S4 Fig**). As expected, EGFP-HBx
167 solubility without the recognition sequence "L" was unaffected by RS-mTEV co-expression
168 (**Fig 2a**). These results clearly demonstrated that RS-mTEV increased the protein solubility
169 via its specific binding to the "L" tag in L-EGFP-HBx *in vivo*. Western blot analysis of the
170 substrate proteins using an anti-GFP antibody was in accordance with their corresponding
171 expression patterns on the above sodium dodecyl sulfate polyacrylamide gel electrophoresis
172 (SDS-PAGE) results. We then investigated the folding quality of the proteins solubilized by
173 RS-mTEV co-expression by measuring EGFP fluorescence intensity in soluble fractions
174 containing the substrate proteins. Solubility enhancement or aggregation inhibition, as
175 important elements for biological relevance, does not necessarily represent proper folding.
176 We observed correlations between EGFP fluorescence intensity and L-EGFP-HBx solubility
177 resulting from RS-mTEV co-expression (**Fig 2a**), indicating that RS-mTEV promoted both
178 solubility and folding of its client protein. The results (**Fig 2a**) revealed that RS-mTEV
179 exhibits the intrinsic chaperone activity.

We further investigated the dosage effects of co-expressed RS-mTEV on L-EGFP-HBx solubility and folding. The increased amounts of co-expressed RS-mTEV protein with increasing L-arabinose concentration (0 %, 0.0022%, 0.0066%, and 0.02%) promoted both L-EGFP-HBx solubility and EGFP fluorescence in an RS-mTEV dosage dependent manner (**Fig 2b**). By contrast, the increase in RS co-expression had no effect on L-EGFP-HBx solubility and EGFP fluorescence under the same condition (**Fig 2b**). These results (**Fig 2**) showed that RS-mTEV was readily converted into a potent chaperone *in vivo* if simply connected to an aggregation-prone protein *in trans*.

RS-mTEV acts as a chaperone independently of the recognition-tag position

One of the advantages of our artificial chaperone system is that the position of the recognition tag in the substrate proteins can be changed. The intrinsic chaperone activity of RS-mTEV led us to predict that RS-mTEV should act as a chaperone, independently of the position of the recognition tag in the substrate proteins. To test this scenario, the "L" tag was placed either in the middle between EGFP and HBx (EGFP-L-HBx) or at the C-terminus of the protein (EGFP-HBx-L). RS-mTEV co-expression increased the solubility of both EGFP-L-HBx and EGFP-HBx-L (from 49% to 86% and from 12% to 73%, respectively) (**Fig 3**). Consistently, the EGFP fluorescence intensity of the substrate proteins in the soluble fractions was positively correlated with their solubility (**Fig 3**). These results have shown that RS-mTEV acts as a chaperone for its substrate proteins independently of the recognition-tag position, giving further credence to the intrinsic chaperone activity of RS-mTEV. In the cases of L-EGFP-HBx and EGFP-L-HBx, we do not know whether RS-mTEV acted co- or post-translationally. EGFP-HBx-L clearly indicated that RS-mTEV acted at least post-translationally, thereby broadening the generality of our system.

RS-mTEV is more efficient than the classical chaperones.

The representative chaperones, including GroEL-GroES (GroELS), the DnaK-DnaJ-GrpE system (DnaKJE), and TF, have been well known to prevent aggregation and assist protein folding in *E. coli* [7, 9, 26]. Here, we compared RS-mTEV chaperone activity with that of these classical chaperones for L-EGFP-HBx, EGFP-HBx-L, and EGFP-HBx proteins. When co-expressed individually with RS, RS-mTEV, GroELS, DnaKJE, and TF, the corresponding solubility of the 3 substrate proteins were observed to be 16%, 72%, 20%, 81%, and 64% for L-EGFP-HBx, and 12%, 71%, 16%, 82%, and 41% for EGFP-HBx-L, and 10%, 9.8%, 14%, 86%, and 33% for EGFP-HBx (**Fig 4a and c**). The co-expression of the chaperones was confirmed (**S5 Fig).** The results showed that, like RS-mTEV, DnaKJE and TF substantially increased the solubility of L-EGFP-HBx and EGFP-HBx-L to the similar levels, whereas GroELS increased little, similar to RS. Furthermore, the EGFP fluorescence intensities of the soluble extracts were correlated with the corresponding solubility of the target proteins upon co-expression with each chaperone, except for DnaKJE (**Fig 4b**). TF increased both the solubility and folding of client proteins more efficiently than GroELS and DnaKJE. Notably, RS-mTEV was shown to be similar to TF regarding the chaperone activity.

We additionally compared the solubility-enhancing effects of RS-mTEV with the representative chaperones for different substrate proteins, including human endostatin, granulocyte colony stimulating factor (GCSF), AP-1 complex subunit mu-2 (Ap1m2), and malate dehydrogenase (hMDH) with the “L” tag at their N-termini. These aggregation-prone proteins have been known to be involved in cell proliferation or signaling pathways [44-47]. Upon individual co-expression of RS, RS-mTEV, GroEL/ES, DnaKJE, and TF, the corresponding solubility were 5%, 47%, 14%, 28%, and 11% for endostatin; 44%, 85%, 53%, 87%, and 94% for GCSF; 7%, 70%, 13%, 36%, and 32% for Ap1m2; and 22%, 79%, 50%, 52%, and 39% for hMDH, respectively (**Fig 4a and c**). These results showed that RS-mTEV

230 robustly increased the solubility of all tested proteins, and that its solubility-enhancing
231 activity was higher than or similar to that of the representative chaperones. In contrast to the
232 substrate preferences of the classical chaperones, RS-mTEV provided the chaperone function
233 for all client proteins tested. The overall results (**Fig 4**) indicate that RS-mTEV is more
234 efficient than the classical chaperones.
235
236 **RS-mTEV chaperone activity largely results from RS rather than mTEV.**
237 As described in Introduction, the substrate-stabilization against aggregation by the surface
238 charges of HSP90, the N-terminal domain of HSP70, and the intermolecular repulsive (or
239 destabilizing) forces of soluble macromolecules appear to act allosterically; long-range
240 chaperone effects exist even in the absence of direct contact with the aggregation-prone
241 regions of the connected polypeptides. This (apparent) allosteric mechanism underlies the
242 concept of the intrinsic chaperone activity of soluble cellular macromolecules. One would
243 therefore expect that RS-mTEV chaperone activity might be mediated by RS after RS-mTEV
244 binding to the "L" tag of client proteins. To test this, we investigated and compared the
245 chaperone effects of three proteins (mTEV without fusion, N-mTEV [N: N-terminal domain
246 (15 kDa) of RS], and RS-mTEV) on L-EGFP-HBx solubility and folding at low-temperature
247 (25 °C), where the solubility of all three proteins is high (**Fig 5a**). Although the three proteins
248 share the same substrate-binding module (mTEV), RS-mTEV was superior to mTEV and N-
249 mTEV at promoting L-EGFP-HBx solubility, whereas N-mTEV chaperone activity was
250 slightly higher than that of mTEV (**Fig 5b and d**). To further confirm RS-mediated
251 chaperone activity, we used a more soluble TEV variant (TEVsw) [48] harboring the same
252 mutation in the TEV domain to block protease activity, yielding mTEVsw. The mTEVsw
253 without fusion was highly soluble, even at 37 °C (**Fig 5a and S1 Fig**). Despite the increased
254 solubility of mTEVsw relative to mTEV, mTEVsw without the RS fusion failed to show

detectable chaperone activity for L-EGFP-HBx, whereas RS-mTEVsw consistently increased L-EGFP-HBx solubility (**Fig 5c and d**). The significant amounts of both mTEV and mTEVsw were observed to co-precipitate with L-EGFP-HBx (**Fig 5b and c**). Consistent with the aforementioned allosteric mechanisms, our findings indicate that RS-mTEV chaperone activity results largely from RS rather than mTEV, although mTEV is critical for the substrate binding. Conversely, both the attractive interactions between mTEV module and L-EGFP-HBx and the probable conformational changes of L-EGFP-HBx by the attractive interactions cannot be sufficient to describe the RS-mediated allosteric chaperone effect.

***In vitro* refolding experiments support RS-mTEV chaperone function**.

To characterize RS-mTEV chaperone function more clearly, *in vitro* refolding experiments using EGFP-HBx-L as a substrate protein were performed in the presence and absence of RS-mTEV. GuHCl-denatured EGFP-HBx-L (80 μM) was 50-fold diluted into the refolding buffer containing 2.5 μM RS-mTEV, RS, or phosphate-buffered saline (PBS), and refolding was monitored by following EGFP fluorescence at various time points (0–75 min) at 30 °C. RS-mTEV increased the final refolding yield by ~ 1. 7 fold high, compared to RS and PBS (**Fig 6a**). Furthermore, consistent with the *in vivo* results (**Fig 2b**), the refolding yields were increased with an RS-mTEV concentration dependence (0–5 μM; **Fig 6b**). By contrast, RS failed to show any detectable chaperone activity, even at the highest concentration tested (**Fig 6a and b**). The final refolding yields of RS-mTEV, RS, and PBS did not converge to the same value (**Fig 6a)**, indicating that the difference in the final fluorescence signals resulted from irreversible aggregation of the substrate proteins. This implies that RS-mTEV likely assisted protein folding by preventing off-pathway aggregation. To confirm this possibility, *in vitro* refolding was performed at substrate concentrations 10-fold lowered (**Fig 6c)**, where intermolecular aggregation was minimized. Under these conditions, RS-mTEV chaperone

activity was substantially attenuated (**Fig 6c**), indicating that RS-mTEV assisted protein folding largely by preventing intermolecular aggregation rather than accelerating the folding rate.

To further confirm *in vitro* RS-mTEV chaperone activity via the specific binding to its canonical recognition sequence in the substrate protein, we investigated the effect of competing peptides on the RS-mTEV chaperone activity. The sequence of the competitive-inhibitor peptide was flanked by TT and GT (TT-ENLYFQS-GT), whereas that of the control peptide represented the inverted form of the canonical recognition sequence (TT-SQFTLNE-GT) harboring a single point mutation in the middle. Addition of the competitive-inhibitor peptide to the refolding buffer abolished RS-mTEV chaperone activity to the level of the control, whereas the control peptide had no inhibitory effect on RS-mTEV chaperone activity (**Fig 6d**). These results demonstrated that *in vitro* RS-mTEV chaperone activity resulted from its specific binding to the canonical recognition sequence.

Discussion

In this study, we have shown that a soluble protein exhibits the intrinsic chaperone activity in terms of aggregation inhibition and folding assistance. A soluble model protein, RS-mTEV, displayed the robust chaperone activity for its client proteins via a specific binding to the "L" tag of 7 residues (**Figs 2a, 3, and 4**). The fluorescence intensity of EGFP-HBx fusion proteins was followed to assess proper folding because of the absence of an *in vitro* HBx assay [49, 50]. In particular, our artificial chaperone system is suitable to explore the intrinsic chaperone activity of a soluble protein due to the following reasons. The "L" tag is very short and located at the "flanking" regions of the client proteins, minimizing the interactions between RS-mTEV and the client proteins, except for the "L" tag. Moreover, RS-mTEV exhibited a high degree of specificity for the "L" tag (**Figs 2a and 6d**), consistent with a previous report [41]. Similar to such separation of the substrate protein into two parts, RS-mTEV comprises two distinct regions, a solubility-enhancing module (RS) and a client-binding module (mTEV), allowing us to distinguish between the contributions of RS and mTEV to the chaperone activity of RS-mTEV (**Fig 5**). The RS-mediated allosteric chaperone activity in RS-mTEV is in a good accordance with the chaperone activity by the surface charges of HSP90 [21] and the N-terminal domain of HSP70 [22]. Consistently, the intrinsic chaperone activity of soluble macromolecules due to their intermolecular steric and electrostatic repulsions appear to act allosterically; soluble macromolecules can act as chaperones without direct attractive interactions with the aggregation-prone regions of their connected polypeptides [4, 23, 37, 39]. All our findings indicate that RS-mTEV exhibits the intrinsic chaperone activity, which is visible, upon binding to the aggregation-prone proteins.

The concept of the intrinsic chaperone activity of a soluble protein can be generally applicable to cellular macromolecules. This highlights the fundamental importance of our findings. Aggregation-prone polypeptides in the crowded cytosol are physically connected to

a variety of cellular macromolecules, including chaperones, through a combination of diverse interactions (covalent/noncovalent, hydrophobic/hydrophilic, transient/permanent, specific/unspecific, direct/indirect, and native/nonnative) [4]. Individual proteins are estimated to continuously interact with the five putative partners in the *E. coli* cytoplasm [51], making quinary interactions with macromolecules inside cells [52]. Our study implies that the above cellular macromolecules potentially act as chaperones for their connected polypeptides irrespective of their connection types. Previously, the intrinsic properties (e.g., excluded volume and surface charges) of soluble proteins and domains were suggested to underlie their robust chaperone activity *in cis* by genetic fusion to aggregation-prone proteins [23]. However, such intrinsic *cis*-acting chaperone activity remains challenging to explore, although it is phenomenologically robust. To facilitate the investigation of such *cis*-acting effects of cellular macromolecules, we initially designed this *trans*-acting system, allowing the independent control of RS-mTEV *in vivo* and *in vitro*. Interestingly, classic chaperones can be converted into potent *cis*-acting solubility enhancers [22, 53, 54], and ribosomes can act as chaperones both in *trans* and in *cis* [27, 34, 55, 56]. Here, RS, a potent solubility enhancer in *cis* [30], provided the *trans*-acting chaperone activity as a component of RS-mTEV (**Fig 5**). All these results show that despite the change in the connection types between the chaperones and their substrates, their chaperone activity persist. Similarly, endoprotease DegP (HtrA) is converted into a chaperone under different conditions [57], with many other protease components previously shown to exhibit chaperone-like activity [58]. Furthermore, various RNAs, highly soluble macromolecules, have been increasingly reported to act as potent chaperones [30, 34, 59-63]. The concept of the intrinsic chaperone activity of the cellular macromolecules in our study can underlie the aforementioned diverse chaperone types. So far, the evolution of the classical chaperones remains largely unknown. Our study

implies that soluble macromolecules including protease mutants can be easily converted into chaperones if they have the ability to bind aggregation-prone proteins.

The (apparent) allosteric effect of RS in RS-mTEV on its client protein (**Fig 5**) might be well explained by intermolecular repulsive (or destabilizing) forces exerted by their excluded volume and surface charge. The allosteric modulation of protein aggregation by cellular macromolecules represents a potential mechanism for intervening in aggregation-associated neurodegenerative diseases, as well as for protein solubility *in vivo*. For example, a bulky protein conjugated to amyloid-specific binding dye dramatically inhibits the amyloid formation due to its steric hindrance or excluded volume repulsion [64], consistent with the intrinsic chaperone activity and the allosteric modulation of RS in RS-mTEV. Our findings imply that the cellular macromolecules that bind to the flanking or remote sites away from aggregation-prone regions in proteins and peptides might be potential drug targets for protein aggregation-associated diseases.

Taken together, the present study on the intrinsic chaperone activity of a soluble protein has a huge impact on the field of chaperones, and provides new insights into the generic chaperoning role of cellular macromolecules, which is associated with the cellular protein folding, aggregation inhibition, proteostasis, aggregation-associated diseases, and protein production technology.

Materials and Methods

Cloning

We used two different types of vectors for co-expression (pGE and pLysE vectors) (**S2 Fig**). The pGE vectors originated from pGE-LysRS [30], and pLysE vectors were obtained from Merck Chemicals GmbH (Novagen; Darmstadt, Germany). First, the pBAD promoter was inserted into the *Nru*I and *Ava*I restriction sites of pLysE, producing the pLysEpBAD vector with a new *Hpa*I site at the flanking regions of the pBAD promoter. We inserted the sequences for RS, RS-mTEV, variants of RS-mTEV, and the molecular chaperones into the pLysEpBAD vector, respectively. Sequences for client proteins, including EGFP-HBx variants, endostatin, GCSF, Ap1m2, and hMDH, were inserted into the *Nde*I and restriction sites in the multi-cloning site (*Hind*III, *Hind*III, *Sal*I, and *Hind*III, respectively) in the presence or absence of the TEV protease-recognition sequence in the pGE vector. The MSEQ amino acid sequence was inserted at the N-terminus of substrate proteins to increase the expression level of proteins (**S6 Fig**).

Protein expression

Competent cells [*E. coli* BL21(DE3)] were co-transformed with the aforementioned vectors, cells were grown, and proteins in the cells were analyzed as previously reported[30], with some modifications. The expression of proteins from the pLysEpBAD vector was induced with 0.02% L-arabinose unless otherwise mentioned, followed by culturing at 25 °C for 1.5 h. Then, the cells were treated with IPTG tailored to the expression of each client protein as follows: 50 μM for EGFP-HBx and hMDH, 75 μM for endostatin, 200 μM for GCSF, and 150 μM for Ap1m2. Cells treated with IPTG were cultured at 25 °C for an additional 4 h. The harvested cells were lysed by sonication in PBS, and target-protein solubility in samples was analyzed by SDS-PAGE. All experiments with error bars were performed in triplicate.

388

389 **Western blot**

390 Lysate samples were loaded onto polyacrylamide gels and transferred to a polyvinylidene
391 difluoride membrane (ISEQ00010; Millipore, Billerica, MA, USA) according to a previously
392 reported protocol[65]. Anti-GFP (632377; Clontech Laboratories, Mountain View, CA, USA)
393 and anti-Penta His (34660; QIAGEN, Hilden, Germany) were used as primary antibodies,
394 and anti-rabbit IgG (A6154; Sigma-Aldrich, St. Louis, MO, USA) and anti-mouse IgG
395 (A4416; Sigma-Aldrich, St. Louis, MO, USA) were used as secondary antibodies.

396

397 **Fluorescence assay of EGFP-fused proteins**

398 The fluorescence of EGFP-HBx variants was measured to investigate the proper folding of
399 proteins. Each soluble fraction of lysed samples was normalized to cellular optical density
400 and added to the well of a 96-well plate (30496; SPL Life Sciences, Gyeonggi-do, Korea).
401 The fluorescent intensity of samples was determined at 485 nm (excitation) and 520 nm
402 (emission), with FLUOstar OPTIMA (BMG Labtech, Cary, NC, USA) used to measure the
403 fluorescence of each well.

404

405 ***In vitro* refolding**

406 Purified EGFP-HBx-L proteins in denaturing buffer [50 mM Tris-HCl (pH 7.5), 300 mM
407 NaCl, 6 M GuHCl, 1 mM DTT, and 1 mM EDTA] were supplemented with 50 mM DTT for
408 30 min before use. The denatured and reduced protein mixtures were 50-fold diluted into
409 refolding buffer [50 mM Tris-HCl (pH 7.5), 150 mM NaCl, and 5 mM $MgCl_2$] and incubated
410 at 30 °C. Different concentrations of RS or RS-mTEV were added to refolding buffer along
411 with 1 mM DTT. For each time-course refolding experiment, four individual samples were
412 prepared for monitoring the refolding reaction as a function of time (0, 15, 45, and 75 min)

where 0 min corresponds to the sample before dilution of denatured proteins into the refolding buffer. After the initiation of the refolding for 0, 30, 60 min, the samples were centrifuged at 15,000 *x g* for 15 min at 30 °C, making the total refolding time 15, 45, and 75 min, respectively. Green fluorescence intensity in the supernatant of each sample was measured. We used RS-mTEVsw for the refolding experiments, which exhibits better stability and solubility than its prototype [48]. When testing 10-fold lower concentrations of EGFP-HBx-L, 1 mg/mL bovine serum albumin was added to the refolding buffer to reduce loss of the substrate protein due to nonspecific adsorption. All refolding experiments were performed in triplicate.

Competitive inhibition of refolding

Peptides (5 mM; TT-ENLYFQS-GT and TT-SQFTLNE-GT) were dissolved in 100% dimethyl sulfoxide and used to inhibit the chaperone effect of RS-mTEV in *in vitro* refolding assays.

Electrophoretic mobility shift assay (EMSA)

Serially diluted and purified RS-mTEV, RS-mTEVsw, and RS-mTEV(N171A) were mixed with 2.5 μM of purified EGFP-L. They were then incubated at room temperature for 30 min and separated on Native-PAGE gel. Before staining with Coomassie brilliant blue (EBP-1011; Elpis Biotech, Daejeon, Korea), a fluorescence image of the gel was captured.

Statistical analysis

The error bars in each graph represent the mean ± standard deviation of results obtained from triplicate experiments. Statistical significance was analyzed using Student's *t* test. A two-tailed P-value was considered statistically significant at $P < 0.05$.

438

439 **Data availability**

440 All data generated or analyzed during this study are included in this published article (and its

441 supplementary information files).

442

443 ## Acknowledgments

444 We thank Helena Berglund for kindly providing the plasmid encoding an engineered

445 Tobacco Etch Virus protease domain.

446

447 ## Author contributions

448 Conceptualization: Seong Il Choi

449 Formal analysis: Soon Bin Kwon, Hotcherl Jeong, Kyun-Hwan Kim, Baik L. Seong, Seong Il

450 Choi

451 Funding acquisition: Baik L. Seong

452 Investigation: Soon Bin Kwon, Kisun Ryu

453 Methodology: Soon Bin Kwon, Kisun Ryu, Keo-Heun Lim, Seong Il Choi

454 Supervision: Baik Lin Seong, Seong Il Choi

455 Validation: Soon Bin Kwon

456 Visualization: Soon Bin Kwon, Ahyun Son, Seong Il Choi

457 Writing-original draft: Soon Bin Kwon, Ahyun Son, Baik L. Seong, Seong Il Choi

458

459 ## Competing financial interests

460 The authors declare no competing financial interests; details are available in the online

461 version of the paper.

462

References

1. Baldwin AJ, Knowles TP, Tartaglia GG, Fitzpatrick AW, Devlin GL, Shammas SL, et al. Metastability of native proteins and the phenomenon of amyloid formation. J Am Chem Soc. 2011;133(36):14160-3.
2. Tartaglia GG, Pechmann S, Dobson CM, Vendruscolo M. Life on the edge: a link between gene expression levels and aggregation rates of human proteins. Trends Biochem Sci. 2007;32(5):204-6.
3. Balchin D, Hayer-Hartl M, Hartl FU. *In vivo* aspects of protein folding and quality control. Science. 2016;353(6294):aac4354.
4. Choi SI, Kwon S, Son A, Jeong H, Kim KH, Seong BL. Protein folding *in vivo* revisited. Current Protein and Peptdie Science. 2013;14(8):721-33.
5. Chiti F, Dobson CM. Protein Misfolding, Amyloid Formation, and Human Disease: A Summary of Progress Over the Last Decade. Annu Rev Biochem. 2017;86:27-68.
6. Kim YE, Hipp MS, Bracher A, Hayer-Hartl M, Hartl FU. Molecular chaperone functions in protein folding and proteostasis. Annu Rev Biochem. 2013;82:323-55.
7. Hartl FU, Hayer-Hartl M. Molecular chaperones in the cytosol: from nascent chain to folded protein. Science. 2002;295(5561):1852-8.
8. Structural Genomics C, China Structural Genomics C, Northeast Structural Genomics C, Graslund S, Nordlund P, Weigelt J, et al. Protein production and purification. Nat Methods. 2008;5(2):135-46.
9. Agashe VR, Guha S, Chang HC, Genevaux P, Hayer-Hartl M, Stemp M, et al. Function of trigger factor and DnaK in multidomain protein folding: increase in yield at the expense of folding speed. Cell. 2004;117(2):199-209.
10. Apetri AC, Horwich AL. Chaperonin chamber accelerates protein folding through passive action of preventing aggregation. Proc Natl Acad Sci U S A. 2008;105(45):17351-5.
11. Marchenko NY, Marchenkov VV, Semisotnov GV, Finkelstein AV. Strict experimental evidence that apo-chaperonin GroEL does not accelerate protein folding, although it does accelerate one of its steps. Proc Natl Acad Sci U S A. 2015;112(50):E6831-2.
12. Gupta AJ, Haldar S, Milicic G, Hartl FU, Hayer-Hartl M. Active cage mechanism of chaperonin-assisted protein folding demonstrated at single-molecule level. J Mol Biol. 2014;426(15):2739-54.
13. Georgescauld F, Popova K, Gupta AJ, Bracher A, Engen JR, Hayer-Hartl M, et al. GroEL/ES chaperonin modulates the mechanism and accelerates the rate of TIM-barrel domain folding. Cell. 2014;157(4):922-34.
14. Libich DS, Tugarinov V, Clore GM. Intrinsic unfoldase/foldase activity of the chaperonin GroEL directly demonstrated using multinuclear relaxation-based NMR. Proc Natl Acad Sci U S A. 2015;112(29):8817-23.
15. Horowitz S, Koldewey P, Stull F, Bardwell JC. Folding while bound to chaperones. Curr Opin Struct Biol. 2017;48:1-5.
16. Koldewey P, Stull F, Horowitz S, Martin R, Bardwell JCA. Forces Driving Chaperone Action. Cell. 2016;166(2):369-79.
17. Patzelt H, Rudiger S, Brehmer D, Kramer G, Vorderwulbecke S, Schaffitzel E, et al. Binding specificity of Escherichia coli trigger factor. Proc Natl Acad Sci U S A. 2001;98(25):14244-9.

510 18. Ellgaard L, Helenius A. Quality control in the endoplasmic reticulum. Nat Rev Mol
511 Cell Biol. 2003;4(3):181-91.
512 19. Richarme G, Kohiyama M. Amino acid specificity of the Escherichia coli
513 chaperone GroEL (heat shock protein 60). J Biol Chem. 1994;269(10):7095-8.
514 20. Pappenberger G, Wilsher JA, Roe SM, Counsell DJ, Willison KR, Pearl LH. Crystal
515 structure of the CCTgamma apical domain: implications for substrate binding to the
516 eukaryotic cytosolic chaperonin. J Mol Biol. 2002;318(5):1367-79.
517 21. Wayne N, Bolon DN. Charge-rich regions modulate the anti-aggregation activity
518 of Hsp90. J Mol Biol. 2010;401(5):931-9.
519 22. Ryu K, Kim CW, Kim BH, Han KS, Kim KH, Choi SI, et al. Assessment of substrate-
520 stabilizing factors for DnaK on the folding of aggregation-prone proteins. Biochem
521 Biophys Res Commun. 2008;373(1):74-9.
522 23. Kim CW, Han KS, Ryu KS, Kim BH, Kim KH, Choi SI, et al. N-terminal domains of
523 native multidomain proteins have the potential to assist *de novo* folding of their
524 downstream domains *in vivo* by acting as solubility enhancers. Protein Sci.
525 2007;16(4):635-43.
526 24. Ellis RJ, Hartl FU. Principles of protein folding in the cellular environment. Curr
527 Opin Struct Biol. 1999;9(1):102-10.
528 25. Feldman DE, Frydman J. Protein folding in vivo: the importance of molecular
529 chaperones. Curr Opin Struct Biol. 2000;10(1):26-33.
530 26. Maier T, Ferbitz L, Deuerling E, Ban N. A cradle for new proteins: trigger factor at
531 the ribosome. Curr Opin Struct Biol. 2005;15(2):204-12.
532 27. Schimmele B, Grafe N, Pluckthun A. Ribosome display of mammalian receptor
533 domains. Protein Eng Des Sel. 2005;18(6):285-94.
534 28. Waugh DS. Making the most of affinity tags. Trends Biotechnol. 2005;23(6):316-
535 20.
536 29. Wittrup KD. Protein engineering by cell-surface display. Curr Opin Biotechnol.
537 2001;12(4):395-9.
538 30. Choi SI, Han KS, Kim CW, Ryu KS, Kim BH, Kim KH, et al. Protein solubility and
539 folding enhancement by interaction with RNA. PLoS One. 2008;3(7):e2677.
540 31. Brandt F, Etchells SA, Ortiz JO, Elcock AH, Hartl FU, Baumeister W. The native 3D
541 organization of bacterial polysomes. Cell. 2009;136(2):261-71.
542 32. Kaiser CM, Goldman DH, Chodera JD, Tinoco I, Jr., Bustamante C. The ribosome
543 modulates nascent protein folding. Science. 2011;334(6063):1723-7.
544 33. Wruck F, Katranidis A, Nierhaus KH, Buldt G, Hegner M. Translation and folding
545 of single proteins in real time. Proc Natl Acad Sci U S A. 2017;114(22):E4399-E407.
546 34. Choi SI, Ryu K, Seong BL. RNA-mediated chaperone type for *de novo* protein
547 folding. RNA Biol. 2009;6(1):21-4.
548 35. Olsen SN, Andersen KB, Randolph TW, Carpenter JF, Westh P. Role of
549 electrostatic repulsion on colloidal stability of Bacillus halmapalus alpha-amylase.
550 Biochim Biophys Acta. 2009;1794(7):1058-65.
551 36. Ortega-Vinuesa JL, Mart, iacute, n R, iacute, guez A, et al. Colloidal Stability of
552 Polymer Colloids with Different Interfacial Properties: Mechanisms. J Colloid Interface
553 Sci. 1996;184(1):259-67.
554 37. Santner AA, Croy CH, Vasanwala FH, Uversky VN, Van YY, Dunker AK. Sweeping
555 away protein aggregation with entropic bristles: intrinsically disordered protein fusions
556 enhance soluble expression. Biochemistry. 2012;51(37):7250-62.

38. Grana-Montes R, Marinelli P, Reverter D, Ventura S. N-terminal protein tails act as aggregation protective entropic bristles: the SUMO case. Biomacromolecules. 2014;15(4):1194-203.
39. De Los Rios P, Ben-Zvi A, Slutsky O, Azem A, Goloubinoff P. Hsp70 chaperones accelerate protein translocation and the unfolding of stable protein aggregates by entropic pulling. Proc Natl Acad Sci U S A. 2006;103(16):6166-71.
40. Choi SI, Son A, Lim KH, Jeong H, Seong BL. Macromolecule-assisted *de novo* protein folding. Int J Mol Sci. 2012;13(8):10368-86.
41. Phan J, Zdanov A, Evdokimov AG, Tropea JE, Peters HK, 3rd, Kapust RB, et al. Structural basis for the substrate specificity of tobacco etch virus protease. J Biol Chem. 2002;277(52):50564-72.
42. Kapust RB, Waugh DS. Escherichia coli maltose-binding protein is uncommonly effective at promoting the solubility of polypeptides to which it is fused. Protein Sci. 1999;8(8):1668-74.
43. Lee SH, Cha EJ, Lim JE, Kwon SH, Kim DH, Cho H, et al. Structural characterization of an intrinsically unfolded mini-HBX protein from hepatitis B virus. Mol Cells. 2012;34(2):165-9.
44. Hanse EA, Ruan C, Kachman M, Wang D, Lowman XH, Kelekar A. Cytosolic malate dehydrogenase activity helps support glycolysis in actively proliferating cells and cancer. Oncogene. 2017;36(27):3915-24.
45. Folkman J. Antiangiogenesis in cancer therapy--endostatin and its mechanisms of action. Exp Cell Res. 2006;312(5):594-607.
46. Morris KT, Khan H, Ahmad A, Weston LL, Nofchissey RA, Pinchuk IV, et al. G-CSF and G-CSFR are highly expressed in human gastric and colon cancers and promote carcinoma cell proliferation and migration. Br J Cancer. 2014;110(5):1211-20.
47. Pilarsky C, Ammerpohl O, Sipos B, Dahl E, Hartmann A, Wellmann A, et al. Activation of Wnt signalling in stroma from pancreatic cancer identified by gene expression profiling. J Cell Mol Med. 2008;12(6B):2823-35.
48. van den Berg S, Lofdahl PA, Hard T, Berglund H. Improved solubility of TEV protease by directed evolution. J Biotechnol. 2006;121(3):291-8.
49. Slagle BL, Bouchard MJ. Hepatitis B Virus X and Regulation of Viral Gene Expression. Cold Spring Harb Perspect Med. 2016;6(3):a021402.
50. Waldo GS, Standish BM, Berendzen J, Terwilliger TC. Rapid protein-folding assay using green fluorescent protein. Nat Biotechnol. 1999;17(7):691-5.
51. McGuffee SR, Elcock AH. Diffusion, crowding & protein stability in a dynamic molecular model of the bacterial cytoplasm. PLoS Comput Biol. 2010;6(3):e1000694.
52. Mu X, Choi S, Lang L, Mowray D, Dokholyan NV, Danielsson J, et al. Physicochemical code for quinary protein interactions in Escherichia coli. Proc Natl Acad Sci U S A. 2017;114(23):E4556-E63.
53. Basters A, Ketscher L, Deuerling E, Arkona C, Rademann J, Knobeloch KP, et al. High yield expression of catalytically active USP18 (UBP43) using a Trigger Factor fusion system. BMC Biotechnol. 2012;12:56.
54. Kyratsous CA, Silverstein SJ, DeLong CR, Panagiotidis CA. Chaperone-fusion expression plasmid vectors for improved solubility of recombinant proteins in *Escherichia coli*. Gene. 2009;440(1-2):9-15.
55. Kudlicki W, Coffman A, Kramer G, Hardesty B. Ribosomes and ribosomal RNA as chaperones for folding of proteins. Fold Des. 1997;2(2):101-8.

604 56. Sorensen HP, Kristensen JE, Sperling-Petersen HU, Mortensen KK. Soluble
605 expression of aggregating proteins by covalent coupling to the ribosome. Biochem
606 Biophys Res Commun. 2004;319(3):715-9.
607 57. Spiess C, Beil A, Ehrmann M. A temperature-dependent switch from chaperone to
608 protease in a widely conserved heat shock protein. Cell. 1999;97(3):339-47.
609 58. Leonhard K, Stiegler A, Neupert W, Langer T. Chaperone-like activity of the AAA
610 domain of the yeast Yme1 AAA protease. Nature. 1999;398(6725):348-51.
611 59. Docter BE, Horowitz S, Gray MJ, Jakob U, Bardwell JC. Do nucleic acids moonlight
612 as molecular chaperones? Nucleic Acids Res. 2016;44(10):4835-45.
613 60. Horowitz S, Bardwell JC. RNAs as chaperones. RNA Biol. 2016;13(12):1228-31.
614 61. Son A, Choi SI, Han G, Seong BL. M1 RNA is important for the in-cell solubility of
615 its cognate C5 protein: Implications for RNA-mediated protein folding. RNA Biol.
616 2015;12(11):1198-208.
617 62. Kim JM, Choi HS, Seong BL. The folding competence of HIV-1 Tat mediated by
618 interaction with TAR RNA. RNA Biol. 2017;14(7):926-37.
619 63. Kim HK, Choi SI, Seong BL. 5S rRNA-assisted DnaK refolding. Biochem Biophys
620 Res Commun. 2010;391(2):1177-81.
621 64. Gestwicki JE, Crabtree GR, Graef IA. Harnessing chaperones to generate small-
622 molecule inhibitors of amyloid beta aggregation. Science. 2004;306(5697):865-9.
623 65. Jang YH, Cho SH, Son A, Lee YH, Lee J, Lee KH, et al. High-yield soluble expression
624 of recombinant influenza virus antigens from *Escherichia coli* and their potential uses in
625 diagnosis. J Virol Methods. 2014;196:56-64.
626

Figure legends

Fig 1. Experimental design for conversion of a soluble protein into a chaperone. Schematic diagram for the construction of an artificial chaperone system to assess the intrinsic chaperone activity of soluble cellular macromolecules. A TEV protease-domain mutant (mTEV) with no proteolytic activity but the binding ability toward its canonical sequence of 7 residues (denoted as "L"; red bar) was fused to the C-terminus of *E. coli* RS, yielding an artificial chaperone, RS-mTEV. EGFP-HBx harboring "L" tag is a client protein of RS-mTEV.

Fig 2. RS-mTEV exhibits potent chaperone activity upon binding to aggregation-prone proteins in *E. coli*. (**a**) Effect of co-expression of RS-mTEV on the solubility and folding of L-EGFP-HBx. RS-mTEV was co-expressed with L-EGFP-HBx, L(m)-EGFP-HBx, and EGFP-HBx, respectively. As negative controls, mock vector pLysE (Control), RS, RS-mTEV(N171A), L(m)-EGFP-HBx, and EGFP-HBx were used. RS-mTEV(N171A) and L(m)-EGFP-HBx harbor the mutations in mTEV and "L" tag, respectively, critical to the substrate protein recognition. Proteins were expressed at 25 °C. The total lysate (T), soluble fraction (S), and pellet (P) of each sample were subjected to SDS-PAGE and western blot analyses. Both solubility on SDS-PAGE and the fluorescence intensity of the EGFP fusion proteins in each soluble fraction were measured and compared. The same analytical methods were used for the following Figs 3-5. Throughout this paper, black and red arrows indicate artificial chaperones (equivalent or control) and substrate proteins, respectively. (**b**) RS-mTEV concentration-dependent chaperone activity. RS-mTEV co-expression was controlled by different concentrations (0–0.02%) of L-arabinose. RS was used as a control.

651

652 **Fig 3. RS-mTEV acts as a chaperone, independently of the recognition tag-position.** The
653 "L" tag was placed either in the linker region between EGFP and HBx (EGFP-L-HBx) or at
654 the C-terminus of protein (EGFP-HBx-L). Effect of RS-mTEV coexpression on the solubility
655 and fluorescent intensity of EGFP-L-HBx and EGFP-HBx-L was analyzed as described in
656 Fig. 2. RS was used as a control.

657

658 **Fig 4. Comparison of RS-mTEV with the representative *E. coli* chaperones.** (**a**) Client
659 proteins co-expressed with RS, RS-mTEV, GroELS, DnaKJE, and TF, respectively, were L-
660 EGFP-HBx, EGFP-HBx-L and EGFP-HBx, as well as endostatin, GCSF, Ap1m2, and
661 hMDH. Their expression patterns on SDS-PAGE were highlighted. (**b**) Comparison of EGFP
662 fluorescence of L-EGFP-HBx, EGFP-HBx-L, and EGFP-HBx of the results shown in **a**. (**c**)
663 Comparison of protein solubility of the substrate proteins in **a**.

664

665 **Fig 5. RS-mTEV chaperone activity is largely dependent on RS rather than mTEV.** To
666 distinguish between the contributions of RS and mTEV to the RS-mTEV chaperone activity,
667 the chaperone activities of three proteins (mTEV, N-mTEV, and RS-mTEV) and their
668 corresponding more soluble variants (mTEVsw N-mTEVsw, and RS-mTEVsw) were
669 compared. Here N represents the N-terminal domain of RS. (**a**) Solubility of mTEV, N-
670 mTEV, RS-mTEV, mTEVsw, N-mTEVsw, and RS-mTEVsw at 25 °C and 37 °C. (**b**)
671 Comparison of the chaperone activities of mTEV, N-mTEV, and RS-mTEV for L-EGFP-
672 HBx at 25 °C. The mTEV and its fusion variants are indicated by black arrows, and the red
673 arrow indicates L-EGFP-HBx. (**c**) Comparison of the chaperone activity of mTEVsw N-
674 mTEVsw, and RS-mTEVsw at 25 °C under the same conditions as described in **b**.

675 Highlighted bands below main SDS-PAGE data in **b** and **c** represent mTEV and mTEVsw,
676 respectively. (**d**) Solubility and fluorescence intensity of each sample in **b** and **c**.

677

678 **Fig 6. Characterization of the chaperone function of RS-mTEV *in vitro*.** (**a**) Refolding
679 kinetics of EGFP-HBx-L (1.6 μM) in the presence of RS-mTEV (2.5 μM) was monitored as a
680 function of time (0, 15, 45, and 75 min). RS and PBS buffer were used as controls. (**b**) Dose-
681 dependent effects of RS-mTEV on EGFP-HBx-L refolding. EGFP fluorescence of the
682 refolded proteins at concentration (0–5 μM) of RS-mTEV (or RS) was measured at 75 min
683 after initiation of refolding. (**c**) Loss of RS-mTEV chaperone activity at 10-fold lower
684 substrate concentrations as compared with those in **a**. (**d**) Specific inhibitory effect of the
685 peptide on RS-mTEV chaperone activity. Refolding experiments were similar to those
686 described in **b**, except for the presence of competing (L) or non-competing [L(m)] peptide.

687

Supporting information

S1 Fig. Expression of mTEV and its derivatives in *E. coli*. mTEV, N-mTEV, and RS-mTEV were expressed in *E. coli* at 25 °C and 37 °C. N and RS represent the N-terminal domain of *E. coli* LysRS and the whole LysRS, respectively. More soluble mTEV variant (mTEVsw) and its derivative (RS-mTEVsw) were also expressed in *E. coli* at 37 °C. The solubilities of the three mTEV variants expressed at 25 °C were similar, whereas that of mTEV decreased at 37 °C. mTEVsw alone was highly soluble even at 37 °C.

S2 Fig. Diagram of co-expression vectors used for aggregation-prone proteins and artificial chaperones. pGET7 vector used for the expression of aggregation-prone substrate proteins harbors an ampicillin-resistance gene and a pUC19 origin of replication. Protein expression under control of T7 promoter was induced by IPTG. pLysEpBAD used for chaperone expression carries a chloramphenicol-resistance gene and a p15A origin of replication. Expression of artificial chaperones under control the pBAD promoter was triggered by L-arabinose.

S3 Fig. **Interaction of the "L" tag with RS-mTEV, RS-mTEVsw, and RS-mTEV (N171A).** EGFP-L was mixed with varying concentrations of RS-mTEV, RS-mTEVsw, or RS-mTEV (N171A), and then the binding between them was analyzed by mobility shift on native PAGE. Fluorescence images were first obtained (right), and then staining with Coomassie brilliant blue (left) was performed.

S4 Fig. **Mutation of the "L" tag in L-EGFP-HBx alters interaction with RS-mTEV.** A mutation was introduced in the conserved residues of the "L" tag, and the resulting mutant variants [L(m), L(m1), L(m2), and L(m3)] were attached to the N-terminus of EGFP-HBx,

713 respectively. These proteins were co-expressed with RS-mTEV in *E. coli*. Mutated sequences
714 in the "L" tag are indicated in red. Expressed proteins were analyzed by SDS-PAGE and
715 verified by fluorescence (histogram, right).
716
717 **S5 Fig. Confirmation of the expression of RS, RS-mTEV, and molecular chaperones.** RS,
718 RS-mTEV, GroELS, DnaKJE, and TF were expressed in *E. coli*, and their expression was
719 analyzed SDS-PAGE. Each target band is indicated by an arrow. In the case of GroELS, the
720 SDS-PAGE (down) was added to clearly see the expression of groES, a relatively small sized
721 protein, which was run through in the upper SDS-PAGE obtained after a long running time
722 for a good resolution.
723
724 **S6 Fig**. **The N-terminal MSEQ tag increases the expression of the substrate proteins of**
725 **RS-mTEV.** (**a**) EGFP-HBx-L in the presence or absence of this tag was expressed in *E. coli*
726 at 37 °C and induced at various IPTG concentrations (0–40 μM). Total lysates of each sample
727 were analyzed by SDS-PAGE and western blot. Red arrows indicate EGFP-HBx-L
728 expression. (**b**) EGFP-HBx-L in the presence or absence of the tag was expressed in *E. coli* at
729 25 °C (induced by 100 μM IPTG) along with RS or RS-mTEV co-expression, followed by
730 SDS-PAGE analysis.
731

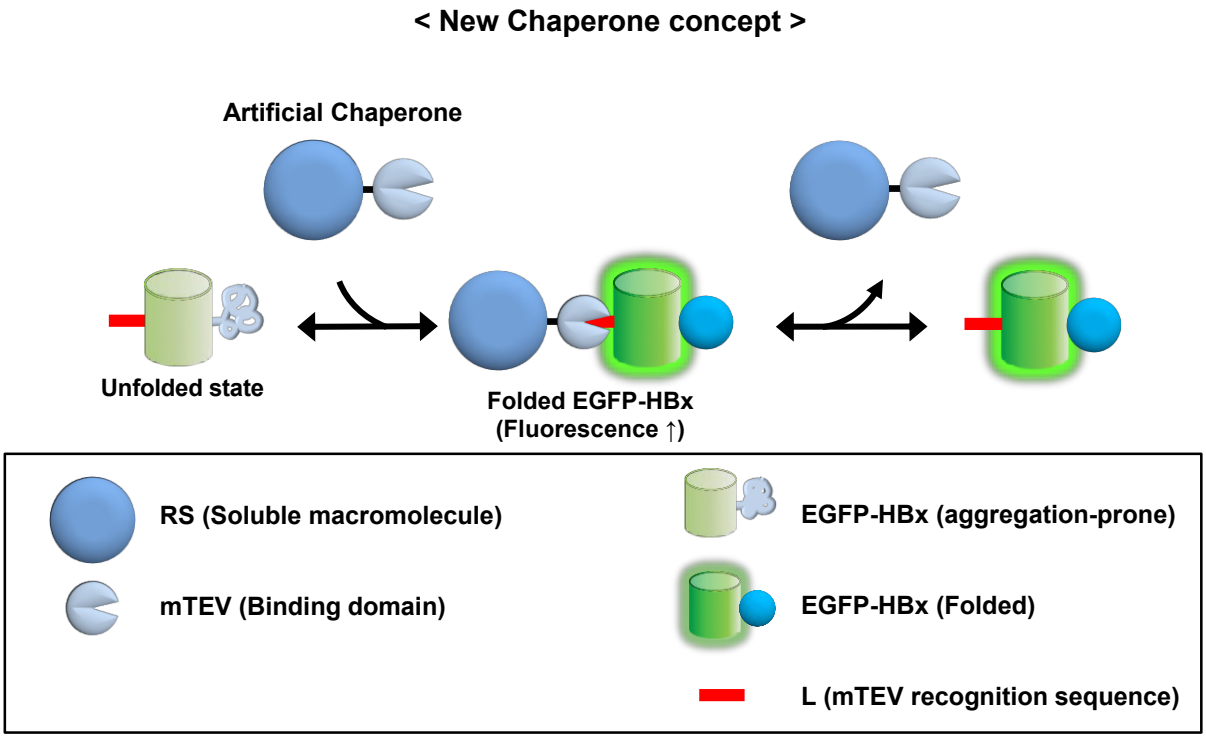

Kwon *et al*. Figure 1.

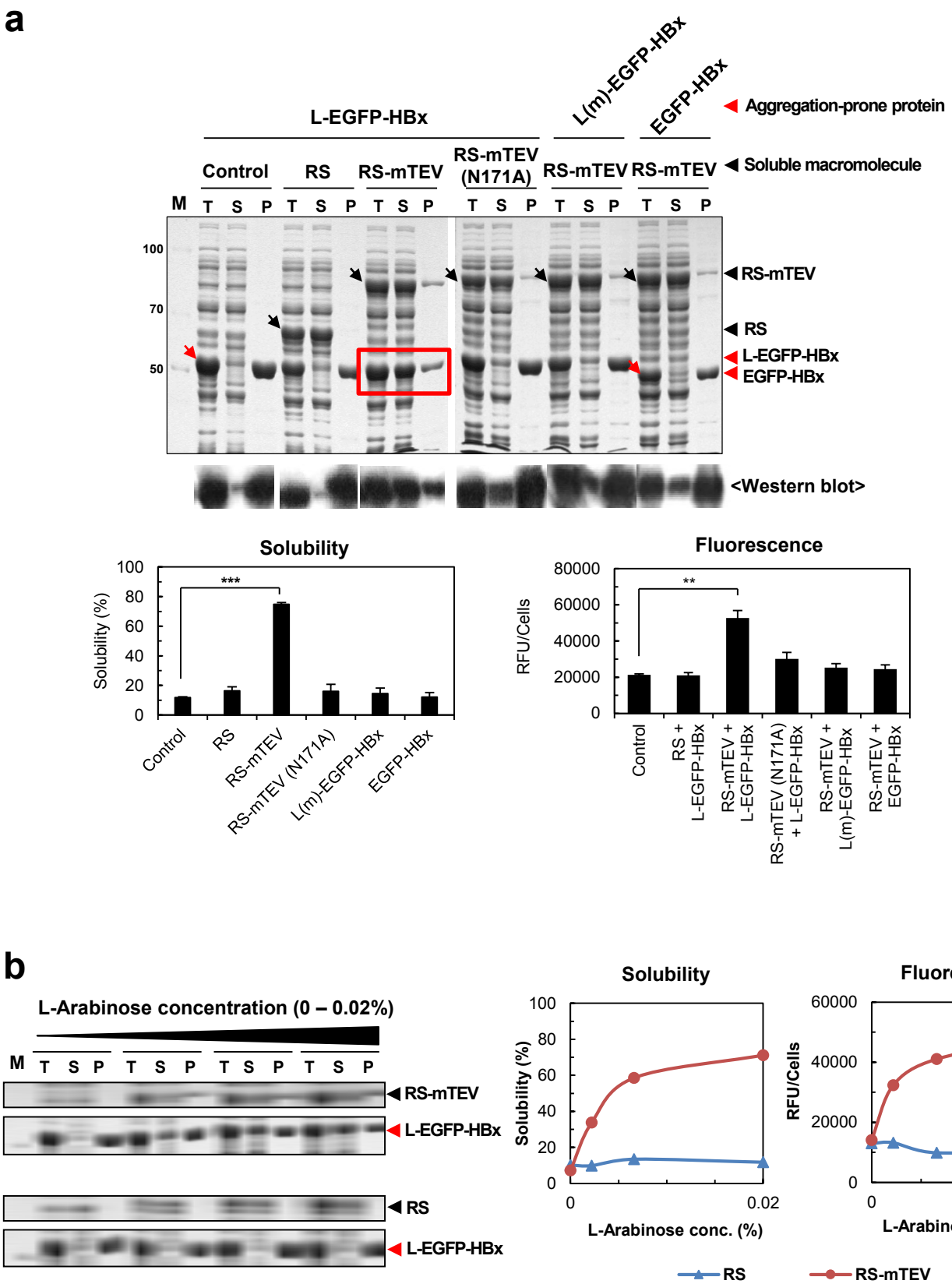

Kwon *et al*. Figure 2.

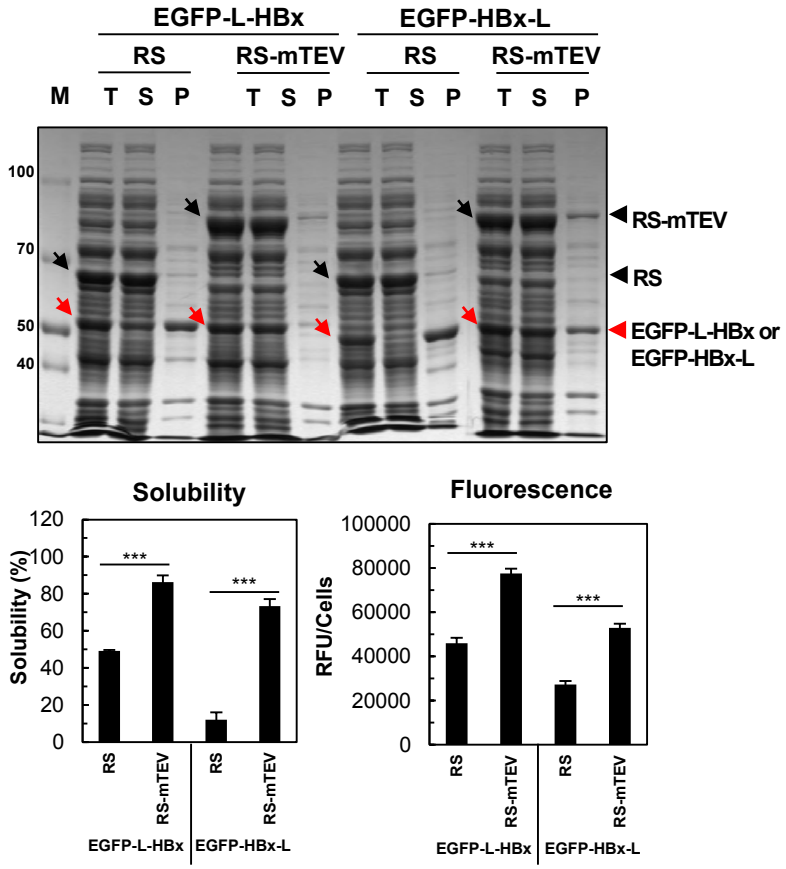

Kwon *et al*. Figure 3.

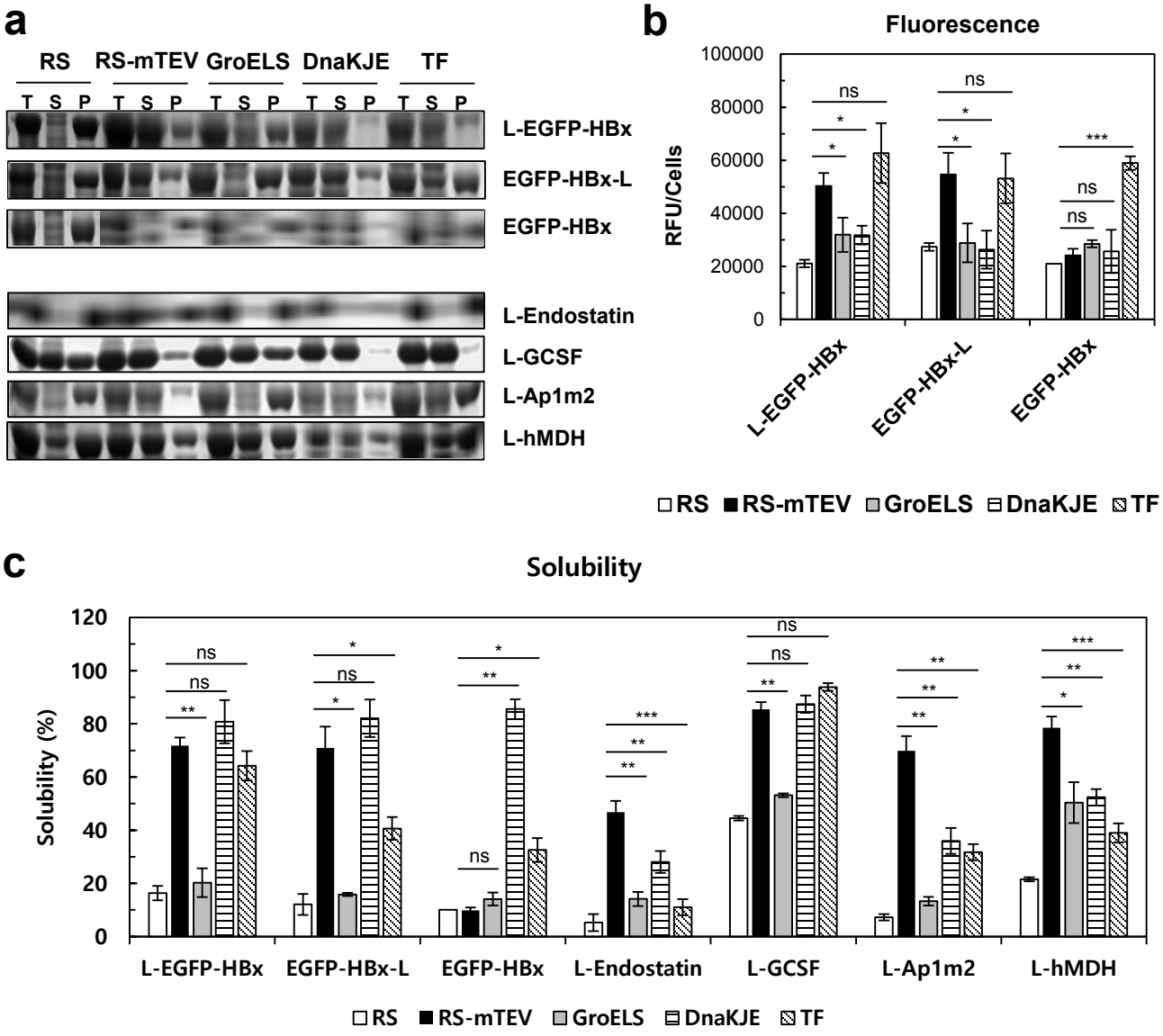

Kwon *et al*. Figure 4.

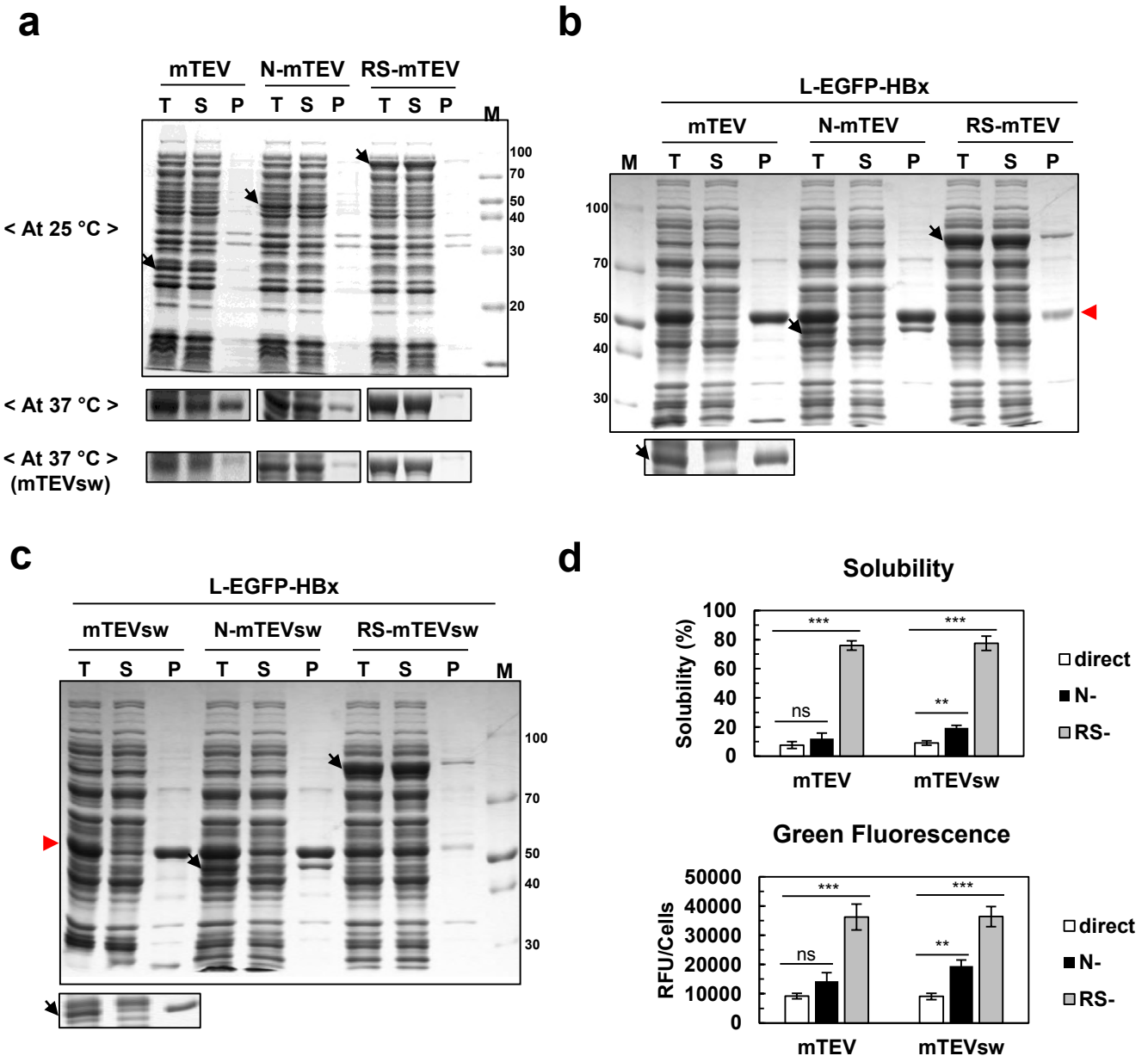

Kwon *et al*. Figure 5.

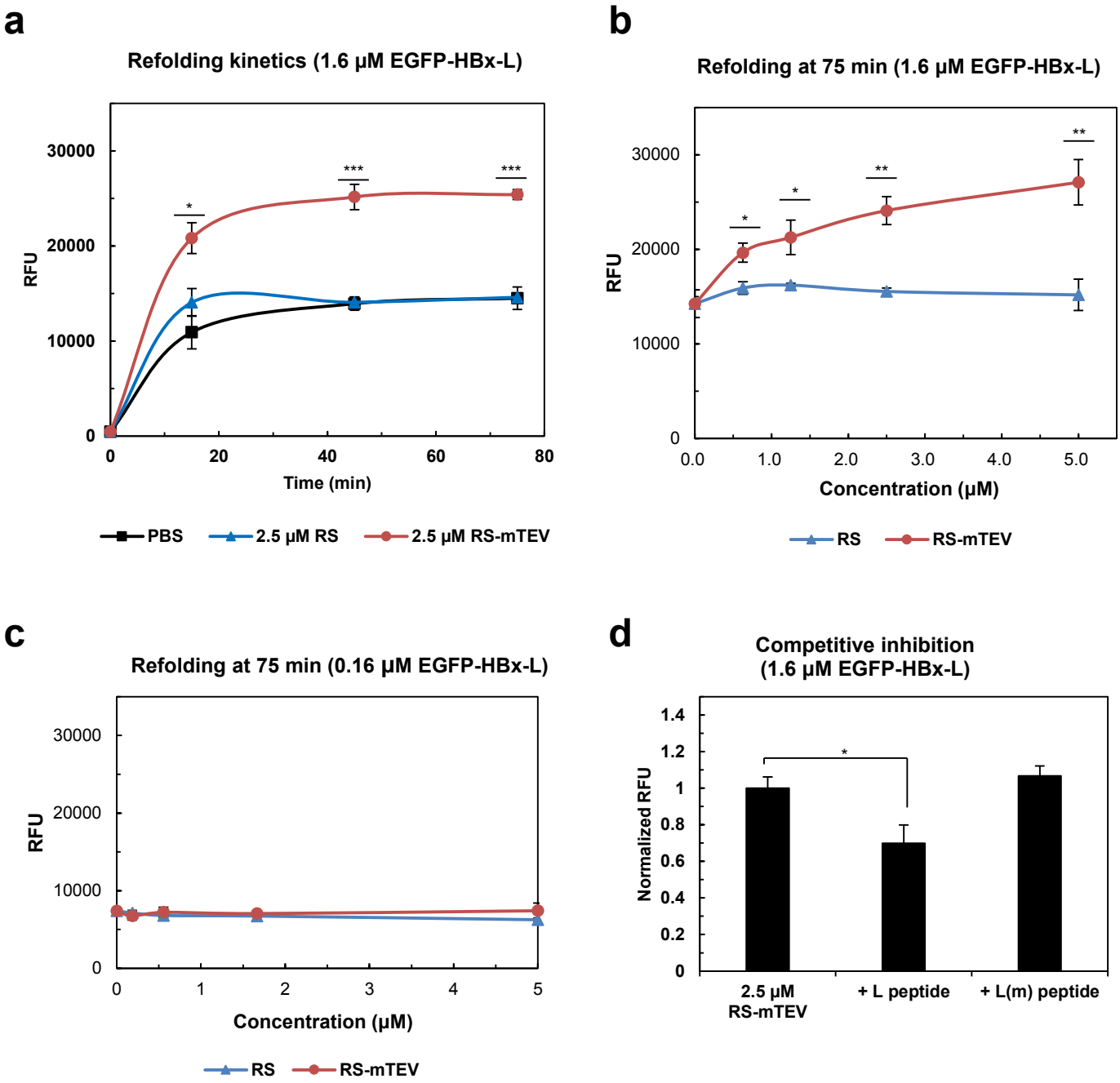

Kwon *et al*. Figure 6.

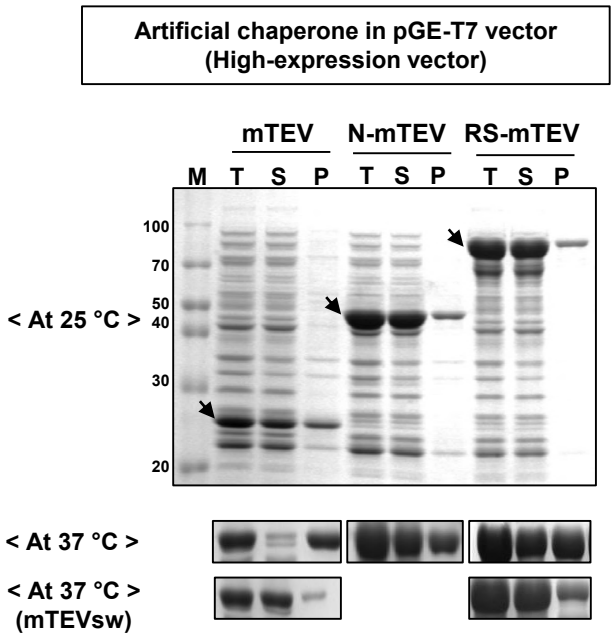

Kwon *et al*. Supplementary Figure 1.

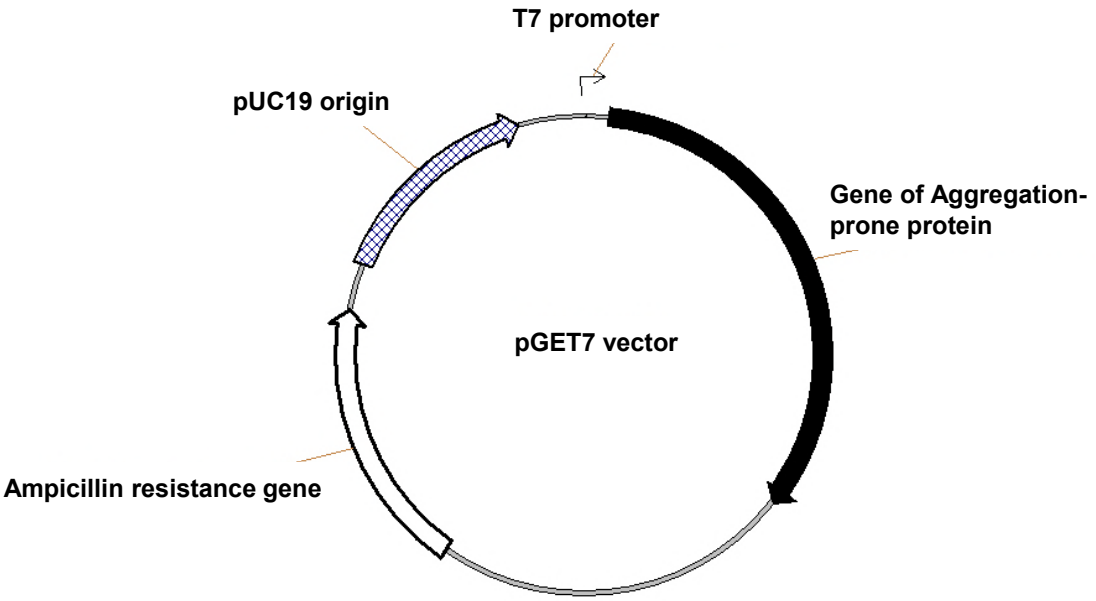

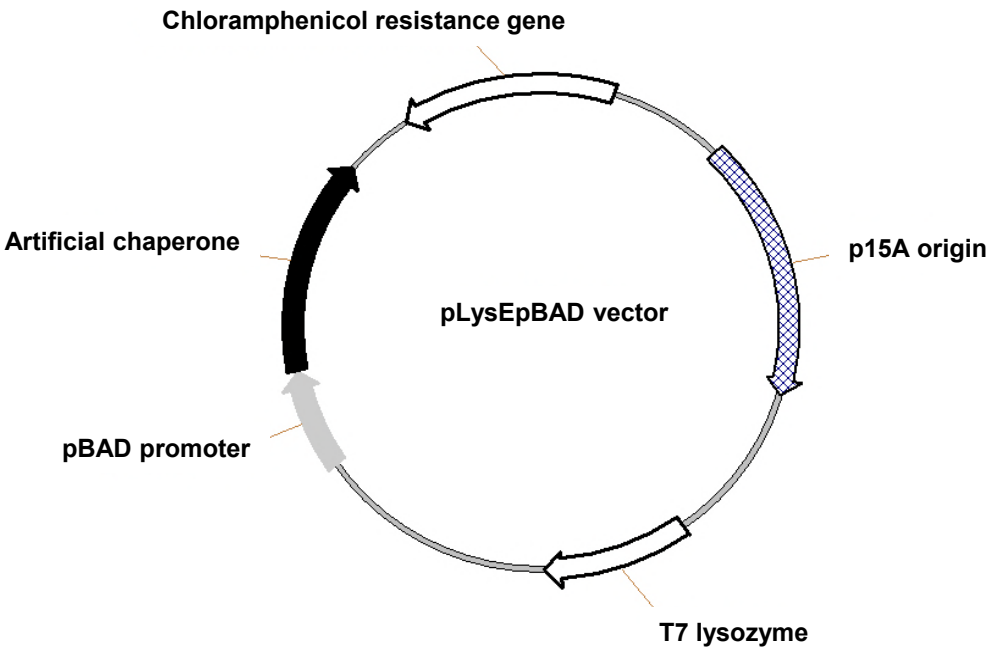

Kwon *et al*. Supplementary Figure 2.

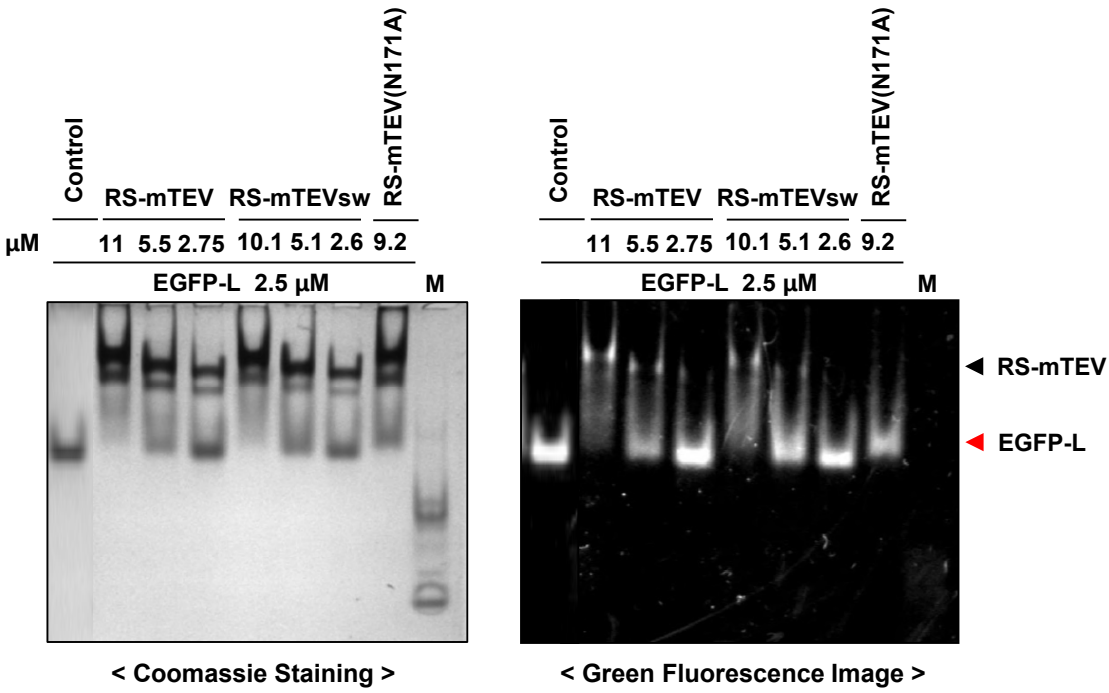

Kwon *et al*. Supplementary Figure 3.

L : ENLYFQG
L(m) : YNLEFQG
L(m1) : ENLQFYG
L(m2) : YNLQFEG
L(m3) : QNLEFYG

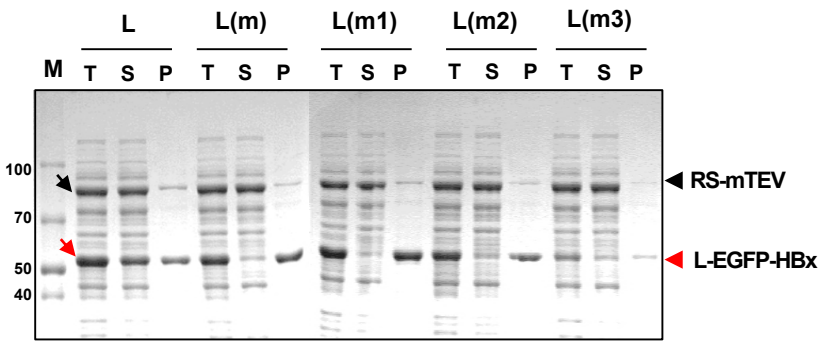

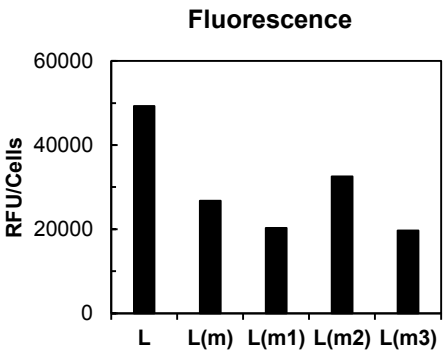

Kwon *et al*. Supplementary Figure 4.

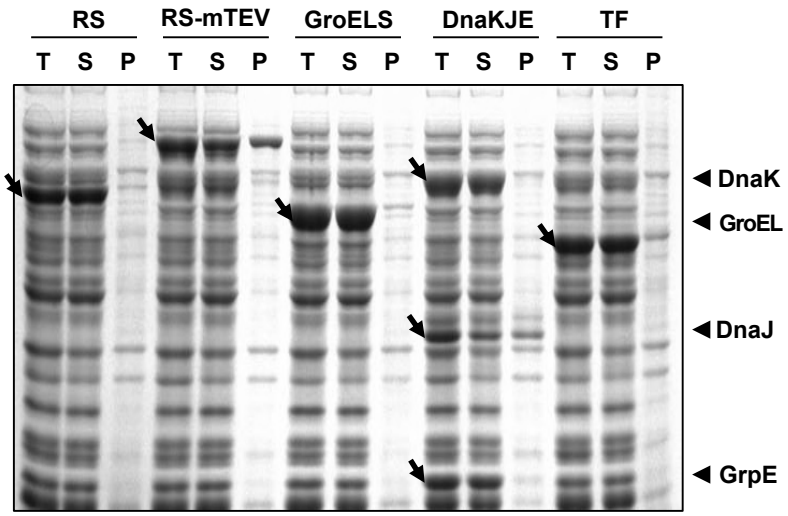

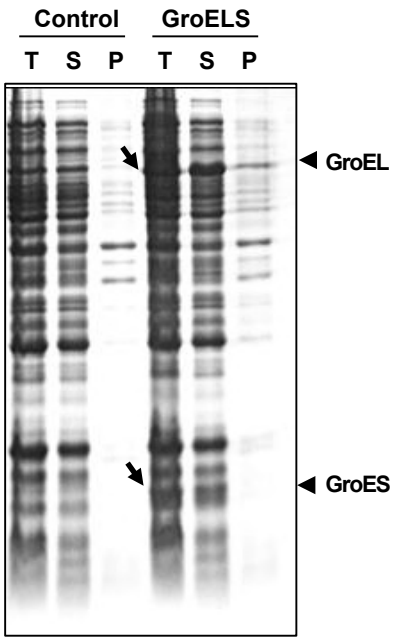

Kwon *et al*. Supplementary Figure 5.

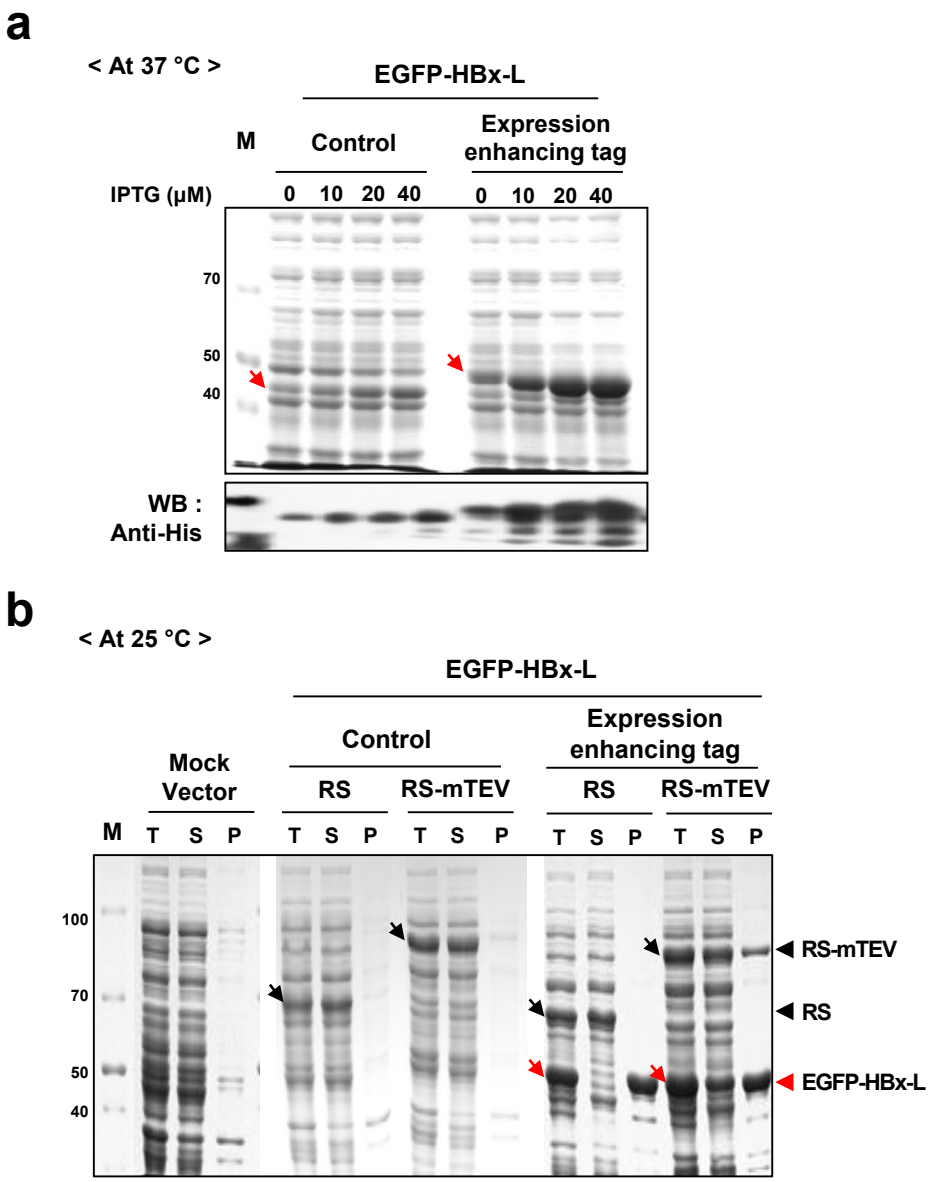

Kwon *et al*. Supplementary Figure 6.